SLAC-PUB-1812
September 1976
(T/E)

DOES ψ PHOTOPRODUCTION CONSERVE HELICITY?*

B. Humpert

Stanford Linear Accelerator Center
Stanford University, Stanford, California 94305

and

Department of Theoretical Physics
University of Geneva, Geneva, Switzerland

A. C. D. Wright†

Stanford Linear Accelerator Center
Stanford University, Stanford, California 94305

ABSTRACT

We suggest the experimental determination of the spin dependence of ψ photoproduction by measuring the decay angular distribution for $\psi \rightarrow \ell^+\ell^-$. Theoretical expectations for the density matrix are explored in the context of several models for ψ photoproduction. In the threshold region, the phenomenological models indicate a substantial breaking of helicity conservation whereas vector-gluon exchange models conserve helicity. Spin measurements can thus provide a test for the gluon exchange approach.

(Submitted to Phys. Lett.)

*Work supported in part by the Energy Research and Development Administration.

†Present address: Dept. of Phys. and Theor. Phys. Inst., University of Alberta, Edmonton, Alberta, Canada T6G 2J1.

In attempting to understand the nature and interaction of the recently discovered ψ particles [1], one is naturally led to compare their properties with those of the lighter vector mesons. Experiments have provided enough data to facilitate comparisons involving decay widths and branching ratios, as well as photoproduction and hadroproduction cross sections [2]. However one kind of experimental information which is available for ρ and ω, namely photoproduction density matrix elements [3], is conspicuously lacking for the ψ's. It is the purpose of the present note to show how the density matrix for photoproduced ψ's can be determined by measuring the decay angular distribution of the leptons in $\psi \to \ell^+\ell^-$, and to investigate the theoretical expectations for the spin dependence of ψ photoproduction. For the latter study, we concentrate on a picture in which the ψ is assumed to be a nonrelativistic bound state of a charmed quark-antiquark pair. In photoproduction, the produced $c\bar{c}$ pair is taken to interact with the nucleon by exchange of two colored vector gluons, as is shown in fig. 1. This "quantum chromodynamics"-type picture for ψ photoproduction is motivated by the charmonium model [4] of the ψ and the Low-Nussinov model [5] for the Pomeron. To put our results in perspective, we also briefly analyse several other models for ψ photoproduction, and compare results for the ψ with those for the ρ.

To begin our discussion of the decay angular distribution [6], we note that $\psi \to e^+e^-, \mu^+\mu^-$ are the largest single ψ decay modes, and can be observed in ψ photoproduction. Therefore, we first discuss the decay angular distribution for $V \to \ell^+\ell^-$ using the formalism of ref. [7]. In the helicity frame of the vector meson this quantity is given by

$$\frac{dN}{d\cos\theta\, d\phi} \equiv W(\theta,\phi) = \sum_{\lambda_V \lambda_V'} \sum_{\lambda_+\lambda_-} \langle \lambda_+\lambda_- | M | \lambda_V \rangle \, \rho_{\lambda_V \lambda_V'} \, \langle \lambda_V' | M^+ | \lambda_+\lambda_- \rangle , \qquad (1)$$

where ρ represents the spin density matrix for the process

$$\gamma(k) + N(p) \rightarrow V(k') + N(p') \quad ,$$

$$\rho_{\lambda_V \lambda_V'} = \frac{1}{N} \sum_{\lambda_N \lambda_\gamma \lambda_{N'} \lambda_\gamma'} T(\lambda_V \lambda_{N'}, \lambda_\gamma \lambda_N)\ \rho_{\lambda_\gamma \lambda_\gamma'}\ T^*(\lambda_V' \lambda_{N'}, \lambda_\gamma' \lambda_N) \ . \tag{2}$$

N is a normalization factor. Assuming that $V \rightarrow \ell^+ \ell^-$ proceeds through a photon, the sum over the lepton and vector meson helicities in (1) leads to the normalized angular distribution

$$\begin{aligned} W(\theta, \phi; \rho(V)) = {} & \frac{1}{2}\left(\rho_{11} + \rho_{-1-1}\right)(1 + \cos^2\theta) + \rho_{00} \cdot \sin^2\theta \\ & + \frac{1}{\sqrt{2}}\left(\mathrm{Re}\,\rho_{10} - \mathrm{Re}\,\rho_{-10}\right) \cdot \sin 2\theta \cdot \cos\phi \\ & - \frac{1}{\sqrt{2}}\left(\mathrm{Im}\,\rho_{10} + \mathrm{Im}\,\rho_{-10}\right) \sin 2\theta \cdot \sin\phi + \mathrm{Re}\,\rho_{1-1} \cdot \sin^2\theta \cdot \cos 2\phi \\ & - \mathrm{Im}\,\rho_{1-1} \cdot \sin^2\theta \cdot \sin 2\phi \ . \end{aligned} \tag{3}$$

It is convenient to form the standard decomposition [7] of $\rho(V)$ in terms of the polarization vector of the photon, $\vec{P}_\gamma$:

$$\rho(V) = \rho^0 + \sum_{\alpha=1}^{3} P_\gamma^\alpha \cdot \rho^\alpha \ . \tag{4}$$

The corresponding decomposition of the decay angular distribution is

$$W(\theta, \phi) = W^0(\theta, \phi) + \sum_{\alpha=1}^{3} P_\gamma^\alpha \cdot W^\alpha(\theta, \phi) \quad , \tag{5}$$

where, from (4), we have

$$\begin{aligned} W^0(\theta, \phi) = {} & \frac{1}{2}\left(1 + \rho_{00}^0\right) + \frac{1}{2}\left(1 - 3\rho_{00}^0\right) \cos^2\theta \\ & + \sqrt{2} \cdot \mathrm{Re}\,\rho_{10}^0 \cdot \sin 2\theta \cdot \cos\phi + \rho_{1-1}^0 \sin^2\theta \cdot \cos 2\phi \quad , \end{aligned} \tag{6a}$$

$$W^1(\theta,\phi) = \rho^1_{11}(1+\cos^2\theta) + \rho^1_{00}\sin^2\theta$$

$$+\sqrt{2}\,\mathrm{Re}\,\rho^1_{10}\cdot\sin 2\theta\cdot\cos\phi + \rho^1_{1-1}\cdot\sin^2\theta\cos 2\phi\ , \tag{6b}$$

$$W^2(\theta,\phi) = -\sqrt{2}\cdot\mathrm{Im}\,\rho^2_{10}\cdot\sin 2\theta\cdot\sin\phi - \mathrm{Im}\,\rho^2_{1-1}\cdot\sin^2\theta\cdot\sin 2\phi\ , \tag{6c}$$

$$W^3(\theta,\phi) = -\sqrt{2}\,\mathrm{Im}\,\rho^3_{10}\cdot\sin 2\theta\cdot\sin\phi - \mathrm{Im}\,\rho^3_{1-1}\sin^2\theta\cdot\sin 2\phi\ . \tag{6d}$$

Note that from (5) the decay angular distribution for photoproduction with unpolarized photons is given by $W^0(\theta,\phi)$. Therefore, information on the density matrix elements ρ^0_{00}, Re ρ^0_{10} and ρ^0_{1-1} can be obtained from experiments with unpolarized photons.

For photoproduction with a linearly polarized beam, one obtains [7]

$$W^L(\theta,\phi,\Phi) = W^0(\theta,\phi) - P_\gamma\cdot\cos 2\Phi\cdot W^1(\theta,\phi)$$

$$- P_\gamma\cdot\sin 2\Phi\cdot W^2(\theta,\phi)\quad , \tag{7}$$

where Φ is the angle between the polarization vector of the photon and the production plane.

What behaviour may be expected for ψ photoproduction density matrix elements? Data [3] for ρ^0 and ω photoproduction at SLAC energies ($s \lesssim 20$ GeV^2, $-t \leq 1$ (GeV/c)^2) are consistent (within 10%) with s channel helicity conservation (SCHC). The diffractive-like s and t dependence of these processes therefore suggests [8] that SCHC is a general feature of diffractive scattering at high energies, as has been borne out in a number of other reactions. Naively one thus might expect SCHC for ψ photoproduction. On the other hand, decay widths, masses and production cross sections differ to such an extent from the corresponding quantities for the lighter vector mesons, that extrapolating from the spin dependence of ρ photoproduction seems highly questionable. Furthermore, at SLAC energies the ψN threshold is nearby; in fact the data [2] for $\sigma(\gamma N \to \psi N)$ show a strong rise near threshold and the onset of the asymptotic region is delayed until $s > 30\ \mathrm{GeV}^2$. Here, we investigate these effects by studying, within the context of several models, the influence of the vector meson mass on the density matrix.

Our interest centers on the above-mentioned QCD picture shown in fig. 1. We are aware that the neglect of multigluon exchange diagrams is not particularly well justified here. Nevertheless we consider it worthwhile to investigate such a picture, particularly since at large $|t|$ the quark-gluon effective coupling constant may be small due to asymptotic freedom [9].

Note that in fig. 1 we have eliminated a loop integration by ignoring the binding of the $c\bar{c}$ pair. According to the nonrelativistic binding, we have partitioned k' equally between the constituents of the ψ. For simplicity, the nucleon is treated as spinless.

Since the external particles are color singlets, the calculation proceeds as in QED, except that, to avoid the infrared problem, we give the gluons a mass m_G. We sketch an outline of the calculation and refer the reader to ref. [10] for details. The amplitudes of fig. 1 are given by

$$T_a = G \cdot \frac{2}{t-m_V^2}\, \bar{u}_2 (\epsilon \cdot k' - \not\epsilon \not k) \not L_a\, v_2 \quad , \tag{8a}$$

$$T_c = G \cdot \frac{2}{t-m_V^2}\, \bar{u}_2 \not L_c (\not k \not\epsilon - \epsilon \cdot k')\, v_2 \quad , \tag{8b}$$

$$T_e = 2 \cdot G \cdot \bar{u}_2 \not L_e v_2 \quad , \tag{8c}$$

where G is a constant. The amplitudes T_b, T_d and T_f are obtained from T_a, T_c and T_e, respectively by the interchange $p_1 \longleftrightarrow -p_2$. The $\not L_j$ ($j = a, \ldots, f$) represent the loop integrals. By use of Feynman parameter integrals, the amplitudes may be cast in the form

$$T_j = G \cdot \frac{2}{t-m_V^2} \int_0^1 (d\alpha)^4 \cdot M_j(p,\alpha) \, \frac{\delta(1-\Sigma\alpha)}{D_j^2} \qquad (j=a,b,c,d) \quad , \tag{9a}$$

$$T_j = 2G \cdot \int_0^1 (d\alpha)^5 \cdot M_j(p,\alpha) \, \frac{\delta(1-\Sigma\alpha)}{D_j^3} \qquad (j=e,f) \quad , \tag{9b}$$

where, for example

$$M_a(p,\alpha) = \bar{u}_2(\epsilon \cdot k' - \not{\epsilon}\not{k}) \not{S}_a \; v_1 \quad . \tag{10}$$

The $\not{S}_j$ are functions of the α_i and the $\not{p}_i$, where p_i is the four-momentum of an external particle. The D_j are the usual denominator functions, and involve the α_i and the invariants of the problem.

In principle the $M_j(p,\alpha)$ could be evaluated exactly; however because of their complexity we have expanded them in powers of s with the help of the algebraic computer program REDUCE. Using well-known techniques [11], we have calculated the remaining parametric integrals to leading order in s, so that all helicity amplitudes are correct to leading order in s. This approximation should be reasonably reliable for s not too near threshold; for example, for ψ photoproduction we take $s \gtrsim 30\ \mathrm{GeV}^2$.

As expected, we find that SCHC holds asymptotically in this model since the nonflip amplitude $T(1,1) \propto s$ whereas the flip-amplitude $T(0,1) \propto$ const. at high energy. We have performed a numerical study for finite s to determine whether SCHC holds near threshold as well. Taking $s = 30\ \mathrm{GeV}^2$ and $m_G = 1$ GeV, we plot ρ^0_{00} for ψ photoproduction (solid line) and ρ photoproduction (dashed line) in fig. 2. The outstanding feature of these results is that <u>SCHC is almost perfectly satisfied</u>. Note, however, that taking $m_G = 0.2$ GeV (dashed-dotted line) significantly changes ρ^0_{00} for ψ photoproduction. Inspection of the helicity amplitudes shows that

Im T(1, 1) vanishes near $m_G = 0.2$ GeV implying that $\rho^0_{00} \approx |T(0, 1)|^2 / |T(1, 1)|^2$ is enhanced. The vanishing of Im T(1, 1) is due to a cancellation between Im T(1, 1) of diagrams (a-d) and Im T(1,1) of diagrams (e, f). The value of m_G at which this occurs is t-dependent. Note that, since photoproduction is not an elastic process, the indefinite sign of Im T(1, 1) does not imply a violation of unitarity.

Although the enhancement appears quite substantial, ρ^0_{00} remains small even at the peak, so that it would be extremely difficult to measure this effect for ψ photoproduction. In principle, measurement of the t dependence of ρ^0_{00} would allow the determination of m_G. However, the main conclusion to be drawn from our study is that SCHC is almost exactly satisfied in this model even near threshold.

For comparison, we have investigated several other models for ψ photoproduction to check whether SCHC near threshold is a general feature. Taking the gluons spinless in fig. 1 results in amplitudes of the same form as in (9), with greatly simplified $M_j(p, \alpha)$ which we have calculated exactly. Taking the parametric integrals to leading order in s shows that SCHC holds asymptotically since $T(1, 1) \propto$ const. while $T(0, 1) \propto s^{-1}$. Nevertheless, as is shown in fig. 3 (curve 4), near threshold SCHC for ψ photoproduction is substantially violated in contrast with vector gluon exchange. Since the $M_j(p, \alpha)$ are calculated exactly in this model, we believe that our results are reasonably accurate even for $s = 20$ GeV^2. As the energy increases, the SCHC limit is rapidly approached. For example, at $s = 200$ GeV^2, $\rho^0_{00} \lesssim 0.01$ for ψ photoproduction.

Finally, we briefly mention two phenomenological models for vector meson photoproduction. In one [12] asymptotic SCHC is put in by hand. However, at $s = 20$ GeV^2 we find that $\rho^0_{00} \approx 0.1$–0.2 for ψ photoproduction, which indicates that threshold effects are substantial (fig. 3, curve 2). Since $s=20\ \mathrm{GeV}^2$ is far from threshold for ρ photoproduction, SCHC is well satisfied for this process. The second phenomenological model [13] was constructed to incorporate many of the properties believed to be relevant in interactions involving currents; however, asymptotic SCHC does not hold exactly in this model. Nevertheless SCHC is almost true numerically, particularly when m_V is large. For ψ photoproduction, threshold effects enhance helicity flip, so that at $s = 20\ \mathrm{GeV}^2$, $\rho^0_{00} \approx 0.1\text{-}0.2$ (fig. 3, curve 3). Our third study involves a model [14] which assumes a Pomeron with scalar spin couplings. From fig. 3 (curve 5) we notice again a substantial deviation from SCHC.

In conclusion, we note that in the ψ-threshold region there is a considerable difference in the pattern of SCHC violation. All phenomenological models, in particular those with scalar 'objects' being exchanged, show substantial violation of SCHC whereas the vector-gluon exchange model, in strong contrast, conserves helicity almost exactly (fig. 3, curve 1). Measurement of the density matrix elements near threshold can therefore provide stringent tests for the existing models and schemes.

Acknowledgements

One of us (B.H.) thanks the Swiss National Science Foundation for financial support, and the other (A.C.D.W.) acknowledges support from the National Research Council of Canada in the form of an NRC Fellowship. Both of us wish to acknowledge the warm hospitality of Professor S. D. Drell and SLAC.

REFERENCES

[1] J. E. Augustin et al., Phys. Rev. Lett. 33 (1974) 1406; C. Bacci et al., Phys. Rev. Lett. 33 (1974) 1408; J. J. Aubert et al., Phys. Rev. Lett. 33 (1974) 1404; G. S. Abrams et al., Phys. Rev. Lett. 33 (1974) 1453. For a review see: B. Humpert, Dynamical concepts on scaling violation and the new resonances in e^+e^- annihilation, Lecture notes in physics 45 (Springer Verlag, Heidelberg 1976).

[2] See for example, G. S. Abrams in Proceedings of the 1975 international symposium on lepton and photon interactions at high energies, Stanford University, edited by W. T. Kirk (Stanford Linear Accelerator Center, Stanford University, Stanford, California 1976), p. 25; R. Prepost, ibid., p. 241; S. C. C. Ting, ibid., p. 155.

[3] J. Ballam et al., Phys. Rev. Lett. 24 (1970) 960; Phys. Rev. D5 (1972) 545; Phys. Rev. D7 (1973) 3150.

[4] T. Appelquist and H. D. Politzer, Phys. Rev. Lett. 34 (1975) 43; E. Eichten et al., Phys. Rev. Lett. 34 (1975) 369.

[5] F. E. Low, Phys. Rev. D12 (1975) 163; S. Nussinov, Phys. Rev. Lett. 34 (1975) 1286; IAS–Princeton report (1975, unpublished).

[6] For an earlier discussion of the decay angular distribution see for example, S. C. C. Ting in Proceedings of the 1967 international symposium on electron and photon interactions at high energies, p. 452.

[7] K. Schilling, P. Seyboth and G. Wolf, Nucl. Phys. B15 (1970) 397.

[8] F. J. Gilman, J. Pumplin, A. Schwimmer and L. Stodolsky, Phys. Lett. 31B (1970) 387.

[9] D. Gross and F. Wilczek, Phys. Rev. Lett. 30 (1973) 1343; H. Politzer, Phys. Rev. Lett. 30 (1973) 1346.

[10] B. Humpert and A. C. D. Wright, to appear.

[11] R. J. Eden, P. V. Landshoff, D. I. Olive and J. C. Polkinghorne, The analytic S-matrix (Cambridge University Press 1966).

[12] P. Dewey and B. Humpert, Nucl. Phys. B33 (1971) 581.

[13] J. W. Moffat and A. C. D. Wright, Phys. Rev. D12 (1975) 765.
Because of a computing error, the model predictions shown in fig. 7 of this paper are incorrect, and the model is in fact in much better agreement with the data.

[14] J. Pumplin and W. Repko, Phys. Rev. D12 (1975) 1376.

FIGURE CAPTIONS

1. Two gluon exchange diagrams for ψ photoproduction.
2. Two vector gluon exchange model predictions for ρ^0_{00} at $s = 30$ GeV^2 plotted versus (-t). Predictions are for ψ photoproduction (solid line) and ρ photoproduction (dashed line) at $m_G = 1$ GeV, and for ψ photoproduction at $m_G = 0.2$ GeV (dashed-dotted line).
3. Predictions for ρ^0_{00} at $s=20$ GeV^2 (dashed lines) and $s=30$ GeV^2 (solid lines). The gluon mass is $m_G = 1$ GeV^2. The models investigated are: (1) vector-gluon exchange, (2) model of ref. [12], (3) model of ref. [13], (4) scalar gluon exchange, and (5) model of ref. [14].

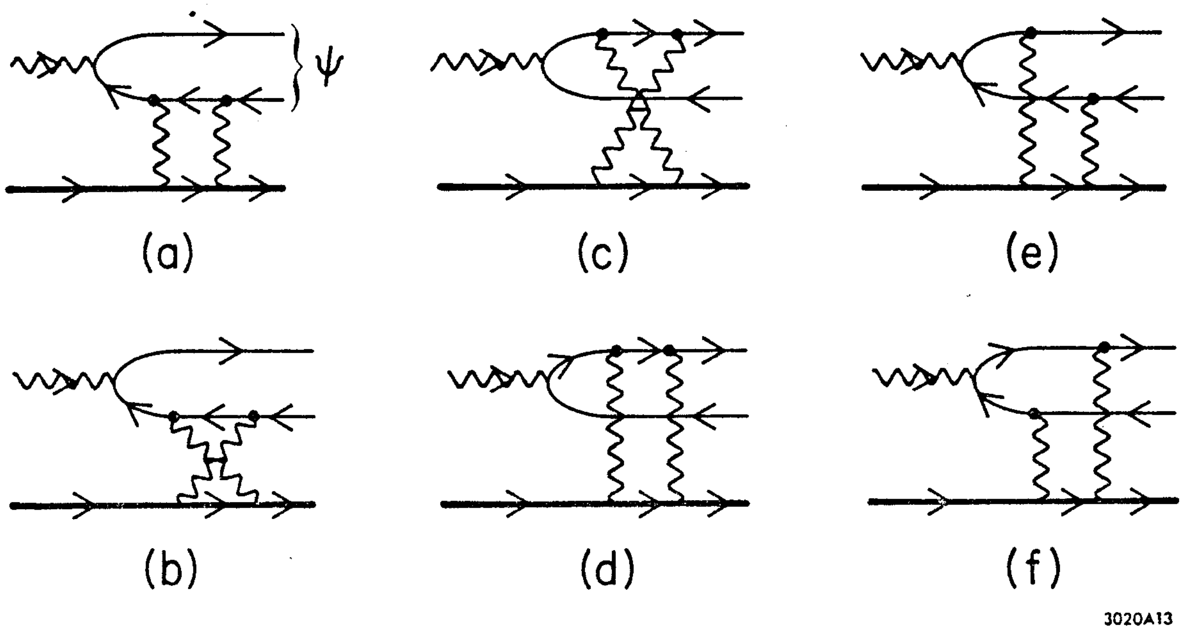

Fig. 1

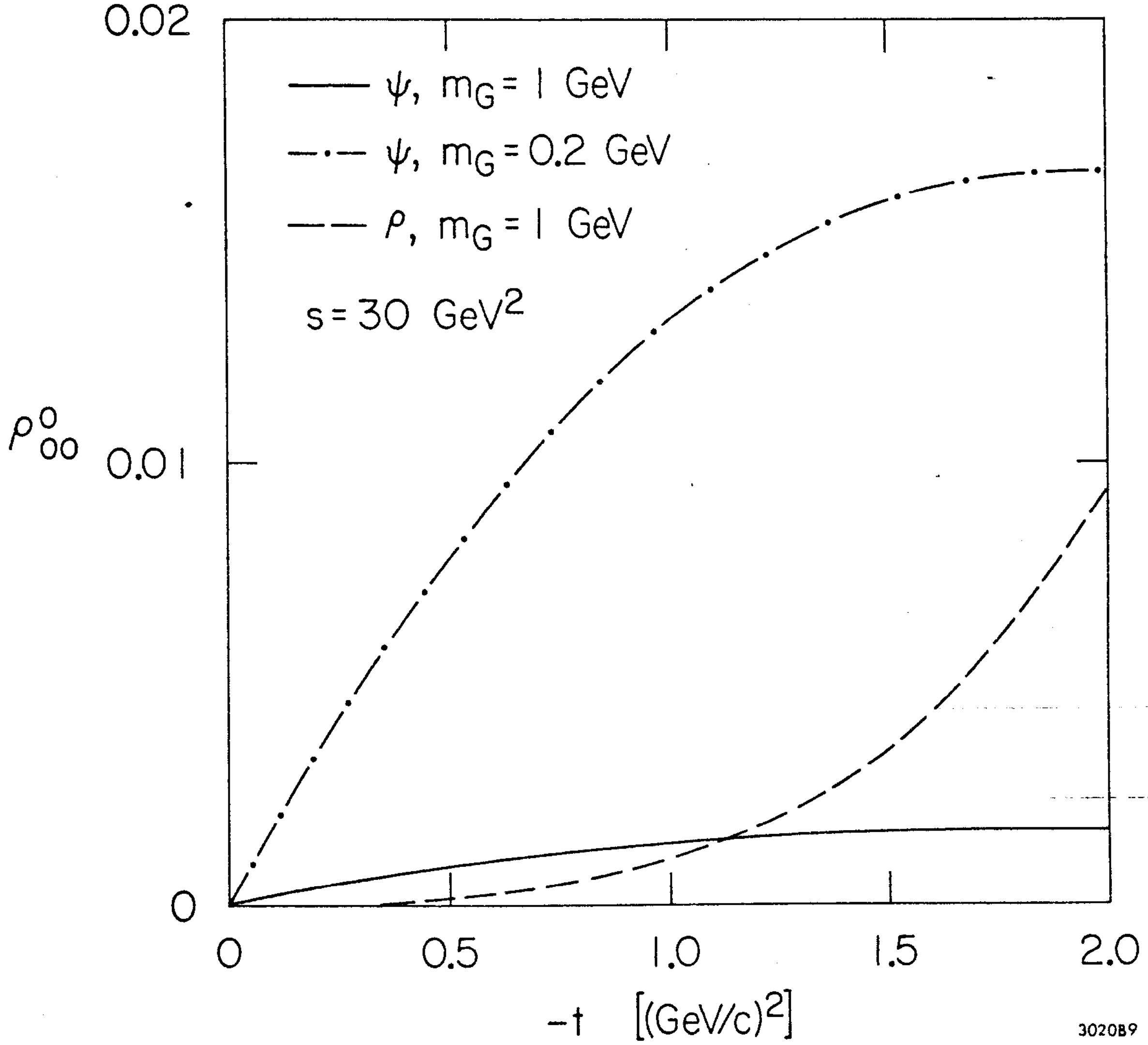

0.02
ψ, m_G = 1 GeV
ψ, m_G = 0.2 GeV
ρ, m_G = 1 GeV
s = 30 GeV^2
ρ^0_{00}
0.01
0
0
0.5
1.0
1.5
2.0
−t [(GeV/c)^2]
3020B9

Fig. 2

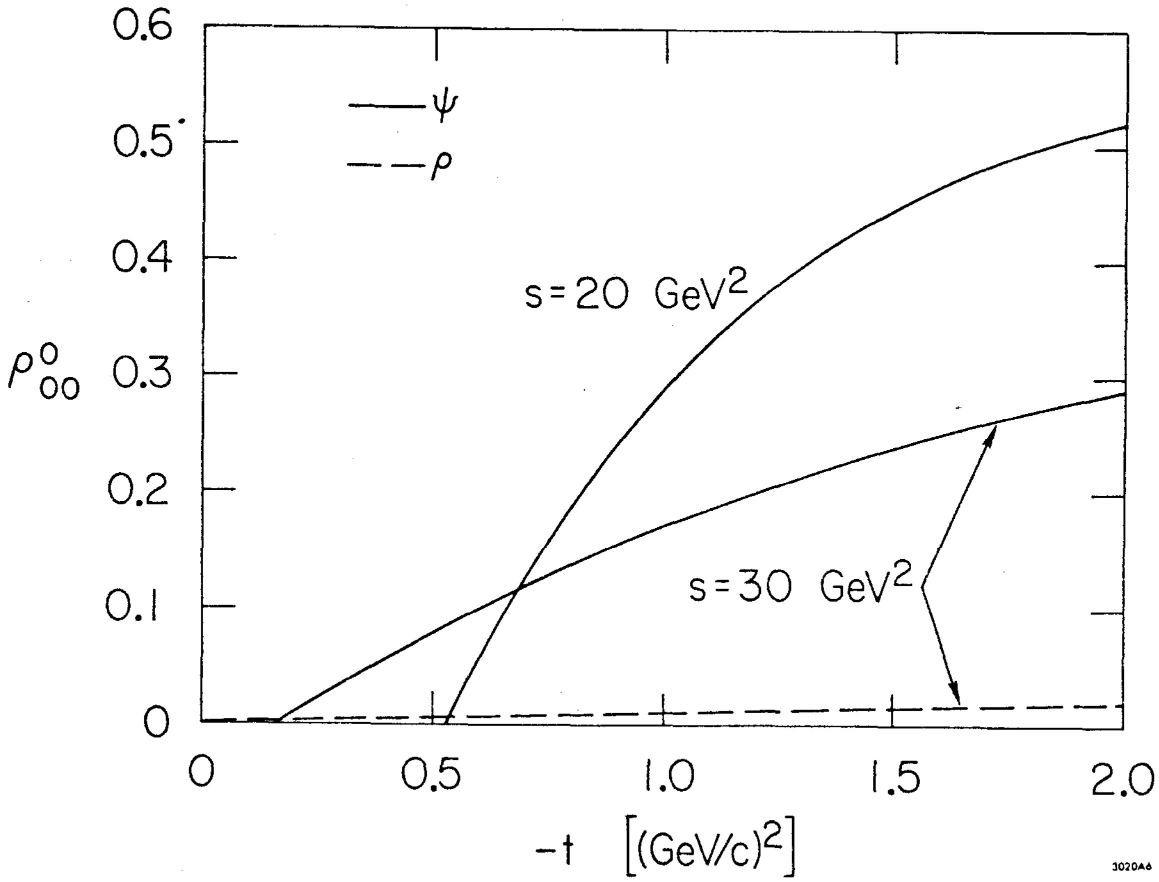

0.6
0.5
0.4
0.3
0.2
0.1
0
ρ^0_{00}
— ψ
-- ρ
s=20 GeV^2
s=30 GeV^2
0
0.5
1.0
1.5
2.0
$-t$ [(GeV/c)^2]
3020A6

Fig. 3